



Astrocyte-Like Cells Derived From Human Oral Mucosa Stem Cells Provide Neuroprotection In Vitro and In Vivo

JAVIER GANZ,^a INA ARIE,^b TAL BEN-ZUR,^a MICHAL DADON-NACHUM,^a SAMMY POUR,^c SHAREEF ARAIDY,^c SANDU PITARU,^b DANIEL OFFEN^a

Key Words. Oral mucosa stem cells • Astrocytes • Cell therapy • Neural differentiation

ABSTRACT

Human oral mucosa stem cells (hOMSC) are a recently described neural crest-derived stem cell population. Therapeutic quantities of potent hOMSC can be generated from small biopsies obtained by minimally invasive procedures. Our objective was to evaluate the potential of hOMSC to differentiate into astrocyte-like cells and provide peripheral neuroprotection. We induced hOMSC differentiation into cells showing an astrocyte-like morphology that expressed characteristic astrocyte markers as glial fibrillary acidic protein, S100 β , and the excitatory amino acid transporter 1 and secreted neurotrophic factors (NTF) such as brain-derived neurotrophic factor, vascular endothelial growth factor, glial cell line-derived neurotrophic factor, and insulin-like growth factor 1. Conditioned medium of the induced cells rescued motor neurons from hypoxia or oxidative stress in vitro, suggesting a neuroprotective effect mediated by soluble factors. Given the neuronal support (NS) ability of the cells, the differentiated cells were termed hOMSC-NS. Rats subjected to sciatic nerve injury and transplanted with hOMSC-NS showed improved motor function after transplantation. At the graft site we found the transplanted cells, increased levels of NTF, and a significant preservation of functional neuromuscular junctions, as evidenced by colocalization of α -bungarotoxin and synaptophysin. Our findings show for the first time that hOMSC-NS generated from oral mucosa exhibit neuroprotective effects in vitro and in vivo and point to their future therapeutic use in neural disorders. STEM CELLS TRANSLATIONAL MEDICINE 2014;3:375–386

INTRODUCTION

Stem cell-based therapy offers promise for future treatment of various neurodegenerative diseases. Two main potential approaches are currently under research. One strategy is cell replacement aimed to substitute lost cells with new cells, as in the case of Parkinson's disease in which lost dopaminergic neurons are replaced with new dopamine-secreting cells [1]. The second approach is to use the cells as vectors that produce and secrete neuroprotective agents or neurotrophic factors (NTF) to provide neuroprotection or trophic stimuli to the surviving neurons. In the nervous system, astrocytes, also called astroglia, play a major neuroprotective role [2]. Recently, malfunction of astrocytes has been proposed to play a role in the pathogenesis of noncell autonomous diseases [3–6]. Recent evidence indicates that NTF-secreting astrocytes support neuronal functional recovery from injuries [2, 7–13].

NTF are naturally occurring polypeptides that support the development, survival, and neurite outgrowth in neurons [14]. Several studies concerning neuronal injury have demonstrated that NTF such as brain-derived neurotrophic factor

(BDNF), vascular endothelial growth factor (VEGF), glial cell line-derived neurotrophic factor (GDNF) and insulin-like growth factor 1 (IGF-1) play an important role in the development, maintenance, and regeneration of the nervous system [7, 15–22]. NTF administration in neuronal dysfunction animal models has been related to axon regeneration and functional recovery [22–25]. Although there are some indications of restoration and recovery of motor function, clinical trials of systemic or intrathecal administration of recombinant NTF to patients with motor neuron disorders did not show significant efficacy, probably due to NTF short half-life, poor delivery, and low concentrations at target sites [26, 27]. Thus, a continuous cellular-derived supply of NTF may overcome this drawback and provide an efficient treatment modality. Our group has previously shown that after a two-step medium-based protocol and without transgenic expression, mesenchymal stem cells can be induced into NTF-secreting cells with astrocyte-like characteristics [18]. After transplantation of these cells, clinical symptoms of multiple sclerosis, Parkinson's disease, Huntington, optic nerve transection, and sciatic nerve injury animal models were significantly attenuated [15, 19, 28–31]. Our

^aNeurosciences Laboratory, Felsenstein Medical Research Center-Rabin Medical Center, Sackler Faculty of Medicine, and ^bOral Biology Department, School of Dental Medicine, Sackler Faculty of Medicine, Tel Aviv University, Tel Aviv, Israel; ^cOral and Maxillofacial Department, Baruch Padeh Medical Center, Poria, Lower Galilee, Israel

Correspondence: Sandu Pitaru, D.M.D., Department of Oral Biology, School of Dental Medicine, Sackler Faculty of Medicine, Tel Aviv University, Israel. Telephone: 972 3 544 4412; E-Mail: pitaru@post.tau.ac.il

Received April 11, 2013; accepted for publication November 4, 2013; first published online in SCTM EXPRESS January 29, 2014.

©AlphaMed Press
1066-5099/2014/\$20.00/0

<http://dx.doi.org/10.5966/sctm.2013-0074>

data demonstrated that these cells increased NTF levels at the injury site and provided an environment that nursed the damaged neuronal tissue.

We recently described a new stem cell population isolated from the neural crest-derived lamina propria of the oral mucosa [32]. This population, termed human oral mucosa-derived stem cells (hOMSC), expresses a primitive neural crest (NC) stem cell phenotype, as evidenced by the expression of the pluripotency transcription factors Oct4, Nanog, and Sox2 and the constitutive expression of the NC markers nestin, Snail, and p75 and the neuronal marker β -III tubulin.

The embryonic NC gives rise to different glial population of the peripheral nervous system (PNS) such as glial satellite cells of the ganglia, enteric glia, and myelinating and nonmyelinating Schwann cells [33]. The task of these glial cells is to provide support to the neuronal cells of the PNS [33, 34]. Moreover, this plasticity is retained postnatal by some differentiated NC-derived cells [34–36]. hOMSC are highly clonogenic and possess the ability to differentiate into NC-derived cell lineages and tissues in vitro and in vivo [32, 36]. Given the multipotency of hOMSC, their NC-related origin, and the fact that during development NC cells gives rise to glial cells, we hypothesized that these cells under the appropriate signaling by soluble factors could serve as a useful stem cell source for autologous cell therapy of neurological disorders. In the present study, we show that hOMSC can acquire an astrocyte-like phenotype characterized by the upregulation of astrocyte markers, enhanced NTF synthesis, and secretion, and consequently by its capability to rescue motor neurons from toxic stimuli in vitro. Most importantly, these cells show the ability to significantly increase the motor performance after sciatic nerve injury in rats and preserve their functional neuromuscular junctions.

MATERIALS AND METHODS

hOMSC Culture

hOMSC were obtained from oral mucosa biopsies performed during routine oral surgical procedures after receiving informed consent from the donors and the approval of the Institutional Helsinki Committee at the Baruch Padeh Medical Center (Poria, Israel). hOMSC were generated and expanded in medium consisting of low-glucose Dulbecco's modified Eagle's medium supplemented with 100 mg/ml streptomycin, 100 U/ml penicillin, 1250 U/ml Nystatin (SPN) (Biological Industries, Beit-Haemek, Israel, <http://www.bioind.com>), 2 mM glutamine (Invitrogen, Carlsbad, CA, <http://www.invitrogen.com>), and 10% fetal calf serum (Gibco, Grand Island, NY, <http://www.invitrogen.com>), as described by Marynka-Kalmani et al. [32]. Briefly, biopsies were incubated at 4°C overnight in dispase (Sigma-Aldrich, Rehovot, Israel, <http://www.sigmaaldrich.com>). Then the epithelial layer was separated from the lamina propria, and the latter was minced into pieces approximately 0.5 mm³. The pieces were placed on the floor of 35-mm culture dishes (Nunc, Rochester, NY, <http://www.nuncbrand.com>). The above-mentioned expansion medium was added gently to the explants to allow their attachment to the floor of the dish. Cells that emigrated from the explant to the culture dishes were harvested with 0.25% trypsin (Biological Industries, Beit-Haemek, Israel) and seeded at a cell density of 4×10^4 cells per 1 cm². Cells were passaged at 70%–80% confluence. hOMSC at passages 4–20 were used in the experiments described below.

hOMSC Differentiation

A two-step medium-based differentiation protocol was performed. In the first step, the cells were incubated in serum-free conditions (Dulbecco's modified Eagle's medium [DMEM] low glucose/SPN/glutamine) with the addition of N2 supplement (Gibco), basic fibroblast growth factor 2 (R&D Systems, Minneapolis, MN, <http://www.rndsystems.com>), and epidermal growth factor (EGF; R&D Systems), all of these supplements at a final concentration of 20 ng/ml. Following 72 hours, the second differentiation step was initiated. Cells were incubated in serum-free medium (DMEM low glucose/SPN/glutamine) with the addition of 1 mM dibutyryl cyclic AMP (Sigma-Aldrich), 0.5 mM 3-isobutyl-1-methylxanthine (IBMX) (Sigma-Aldrich), 50 ng/ml Neuregulin, and 1 ng/ml platelet-derived growth factor (PDGF; Peprotech Asia, Rehovot, Israel, <http://www.peprotech.com>) for an additional 72 hours. For conditioned medium experiments, medium was replaced with serum-free medium after the end of the differentiation protocol and cells were incubated for another 48 hours. Resultant medium was centrifuged to remove cells and debris, and protease inhibitor was added and stored at –80°C until used.

Immunodetection

For immunofluorescence analysis, cells were fixed in 4% paraformaldehyde in phosphate-buffered saline (PBS) and preincubated for 60 minutes in blocking solution (5% goat serum, 1% bovine serum albumin, 0.05% Triton X-100 PBS). Primary antibodies were diluted in the blocking solution and applied overnight at 4°C. Primary antibodies were incubated in blocking solution overnight at 4°C. The following antibodies were used: glial fibrillary acidic protein (GFAP) (1:200; Dako, Glostrup, Denmark, <http://www.dako.com>), S100 β (1:200; Sigma-Aldrich), BDNF (1:100; Santa Cruz Biotechnology, Santa Cruz, CA, <http://www.scbt.com>), GDNF (1:100; Santa Cruz Biotechnology), IGF-1 (Santa Cruz Biotechnology), and VEGF (Santa Cruz Biotechnology). Primary antibodies were detected with fluorescently labeled secondary antibodies Alexa 488 and 568 (1:500; Molecular Probes, Eugene, OR, <http://probes.invitrogen.com>) for 1 hour at room temperature. Nuclear DNA was stained using 4',6-diamidino-2-phenylindole (DAPI) (1:1,000; Sigma-Aldrich). Cells incubated overnight with the blocking solution and then only with the secondary antibodies served as negative controls and for determining the photography exposure settings. Photographs were taken with fluorescence Olympus IX70-S8F2 microscope with a fluorescent light source (excitation wavelength, 330–385 nm; barrier filter, 420 nm) and a U-MNU filter cube (Olympus, Center Valley, PA, <http://www.olympusamerica.com>). Fluorescence quantification was performed by integrated density of fluorescence by ImageJ software (National Institutes of Health, Bethesda, MD, <http://imagej.nih.gov/ij>).

Western Blot Analysis

For Western blot analysis, cells were lysed in buffer containing PBS, 1% SDS, and complete protease inhibitor (Sigma-Aldrich), and loaded into 12% SDS-polyacrylamide gel electrophoresis. Three independent cultures were used as biological replicates. Gels were transferred using liquid transference (300 mA, 1.15hs), and membranes were blocked with PBS buffer/5% milk for 2 hours at room temperature. The membranes were probed with the following antibodies: GFAP (1:500; Invitrogen, Carlsbad, CA), excitatory amino acid transporter 1 (EAAT1) (1:750; Abcam, Cambridge,

U.K., <http://www.abcam.com>), and β -actin (1:1,000; Sigma-Aldrich), and followed by IRDye (680, 800 nm)-conjugated secondary antibody (LI-COR, Lincoln, NE). The membranes were analyzed, and bands were quantified with Odyssey IR imaging systems (LI-COR).

Real-Time Polymerase Chain Reaction

Total RNA was isolated by TRI reagent (Invitrogen), according to the supplier's recommendations. The amount and quality of RNA were determined with the ND-1000 spectrophotometer (NanoDrop, Wilmington, DE, <http://www.nanodrop.com>). For each sample, 2 μ g RNA was used for reverse transcription performed with random primers and SuperScript III (Invitrogen). Real-time semiquantitative polymerase chain reaction (PCR) of the desired genes was performed in an ABI Prism 7700 sequence detection system (Applied Biosystems, Foster City, CA, <http://www.appliedbiosystems.com>) by using PlatinumR SYBR Green qPCRSuperMix UDG with ROX (Invitrogen). PCR amplification was set at 40 cycles (program: 2 minutes at 50°C; 2 minutes at 95°C; 40 repeats of 15 seconds at 95°C and 30 seconds at 60°C). Data were quantified by using the $\Delta\Delta$ cycle threshold method and averaged upon normalization to the glyceraldehyde-3-phosphate dehydrogenase gene. The following primers (IDT, Jerusalem, Israel) were used: lactate dehydrogenase A, 5'-CCATACAGGCACACTGGAATCTC-3' (forward) and 5'-ATCTTGACCTACGTGGCTTGA-3' (reverse); VEGF, 5'-TACCTCCACCATGCCAAGTG-3' (forward) and 5'-GATGATTCTGCCCTCCTCTT-3' (reverse); BDNF, 5'-AGCTCCGGGTTGGTATAC-TGG-3' (forward) and 5'-CCTGGTGGAACTCTTTGCG-3' (reverse); GFAP, 5'-GCCACTGTGAGGAGAAGCT-3' (forward) and 5'-TGGCTTCATCTGCTTCTGTCTA-3' (reverse); EAAT1, 5'-CGAAGCCATCATGAGACTGGTA-3' (forward) and 5'-TCCCAGCAATCAGGAAGAGAA-3' (reverse); p75-NTR, 5'-CGTATCCGACGAGGCCAAC-3' (forward) and 5'-CCACAAGGCCACAACCACAGC-3' (reverse); β -III tubulin, 5'-CTCAGGGGCCCTTTGGACATC-3' (forward) and 5'-CAGGCAGTCGCAGTTTTAC-3' (reverse); neural adhesion molecule (NCAM), 5'-AACCACTCAGACTACATCTGCCAC-3' (forward) and 5'-CCTGTCAATCATGCTGTTGGTG-3' (reverse); octamer-binding transcription factor 4 (OCT-4), 5'-CTTCCCTCAACCAGTTGCCCAAC-3' (forward) and 5'-GACAGGGGGAGGGGAGGAGCTAGG-3' (reverse); NANOG, 5'-TGCTCACACGGAGACTGTC-3' (forward) and 5'-AGTGGTTGTTGCCTTTGG-3' (reverse).

Enzyme-Linked Immunosorbent Assay-Based Measurement of NTF Secretion

At the end of the differentiation process, human VEGF and BDNF concentrations in the cell culture supernatant were measured using a sandwich enzyme-linked immunosorbent assay (ELISA) procedure, according to the manufacturer's instructions (DuoSet; R&D Systems). Medium was processed as conditioned medium (as described above). Briefly, supernatant media samples (100 μ l) were measured in triplicate per flask. The samples were incubated overnight on coated plates, followed by exposure to a second antibody and streptavidin-horseradish peroxidase-based detection (H_2O_2 and tetramethylbenzidine solution). After the addition of the kit stop solution, the absorbance at 450 nm and 570 nm was recorded using a microplate reader. The results (mean \pm SEM) were calculated as secreted protein by 1 million cells per milliliter of medium.

Cell Viability Assay

We have tested the ability of undifferentiated and differentiated hOMSC conditioned media prepared as described above to

protect mouse motor neuron-like hybrid cell line (NSC-34) from hypoxia (2% O_2 , 5% CO_2 , 93% N_2) and oxidative stress (25 μ M H_2O_2). NSC-34 were plated in 96-well plates at 10,000 cells per well and placed in a hypoxic environment for 72 hours in a chamber together with the respective conditioned media. After 72 hours, Alamar blue 10% (AbD Serotec, Kidlington, U.K., <http://www.ab-direct.com>) was added to the cells to quantify viability. The assay was conducted in triplicate, and results were read at wavelengths of 590 nm using a FLUOstar device (BMG Labtech, Offenburg, Germany, <http://www.bmg-labtech.com>). Results were normalized to cells under the same treatments in normoxia. For oxidative stress studies, NSC-34 cells were exposed to 25 μ M hydrogen peroxide (Sigma-Aldrich) and incubated with conditioned media of undifferentiated and differentiated hOMSC for 24 hours. Data were normalized and expressed as percentage of cells present in serum-free conditions with no insult.

Sciatic Nerve Injury and Cell Transplantation

The sciatic nerve crush model was applied on 8-week-old male Sprague-Dawley rats ($n = 24$; Harlan, Jerusalem, Israel, <http://www.harlan.com>), weighing 230–250 g. Rats were housed under 12-hour-light/12-hour-dark conditions and grown in individually ventilated cages with ad libitum access to food and water. All experimental protocols were approved by the Tel Aviv University Committee of Animal Use for Research and Education. Every effort was made to reduce the number of animals used and to minimize their suffering. Two independent experiments of four animals per group were performed. hOMSC derived from a different donor were used in each independent experiment. The results from the two experiments were pooled and presented as the mean \pm SEM/animal. Rats were anesthetized for the sciatic nerve injury and for cell transplantation with chloral hydrate (300 mg/kg; Sigma-Aldrich), and subcutaneous daily cyclosporine (Novartis International, Basel, Switzerland, <http://www.novartis.com>) was given (3.75 mg per rat). The right sciatic nerve was exposed, and a vessel clamp was applied 10 mm above the first branching of the nerve, for 30 seconds. Then the muscle and skin were closed in layers. Twenty-four hours after injury, differentiated hOMSC and naïve cells were harvested, labeled with superparamagnetic iron oxide (5 g/ml; Feridex; Bayer HealthCare, Leverkusen, Germany, <http://www.bayer.com>), centrifuged, resuspended at a concentration of 1×10^6 cells per 100 μ l of saline, and maintained on ice until transplantation. A total of 24 animals was subjected to sciatic nerve injury and then divided into three groups of 8 animals each. Each group was treated with either differentiated hOMSC or naïve hOMSC or saline (control). A total of 100 μ l of cell suspension (1×10^6 cells) or saline was injected through the gastrocnemius muscle into the nerve surroundings and above the first branching of the nerve. To ascertain 98% viability of the cells to be transplanted, trypan blue staining was performed in parallel aliquots obtained from the same cultures from which the cells to be transplanted were obtained. All treated animals were sacrificed 10 days after transplantation for histological examination.

Rat Motor Function Measurements

Motor activity was measured using the San Diego Instrument test, Rotarod (San Diego Instruments, San Diego, CA, <http://www.sandiegoinstruments.com>), between days 1 and 10 after cell transplantation. This test measured the time that the rats remained on a rotating rod in accelerated speed (0–25 rpm). Following a brief training period, adult Sprague-Dawley rats were able to remain balanced on

the rod for up to 4 minutes. After sciatic nerve crush, the rat's ability to balance is severely compromised, causing the animal to fall off the rod after shorter periods of time. The average time measured in three consecutive runs for each rat was recorded, and the group's performance was compared. The machine has a laser beam that detects the fall. The rotarod test was assessed at days -1, 0, 2, 4, 6, and 10 after transplantation. Data are presented as percentage values of each individual (mean [%] \pm SEM) relative to the initial time they spent on the rod before injury.

Assessment of Cell Engraftment, Migration, and Phenotype Maintenance

To analyze cell survival following transplantation, hOMSC were infected with lentiviral particles (Gateway; Invitrogen) carrying the pLenti CMV-GFP-Puro plasmid (Addgene 17448, kindly deposited by Eric Campeau) and selected for puromycin resistance (2 μ g/ml) for 2 weeks. Selected colonies were expanded and submitted to the differentiation protocol described above or maintained in expansion medium. Naïve and differentiated green fluorescent protein (GFP)⁺ cells were transplanted following sciatic nerve injury in 12 animals, as described above, each type of cell in a group of 6 animals. Three animals from each group were sacrificed 4 hours after transplantation. The remaining six animals treated with GFP⁺ cells and the animals used for motor tests were sacrificed 10 days after transplantation with CO₂. The hind limb muscles were removed and frozen in liquid nitrogen. Muscles were sectioned perpendicularly to the long axis of the muscle. Serial sections of 30 μ m were obtained using a cryostat (Leica CM1850) and placed on glass slides for histological and immunohistochemistry staining. Tissue sections of animals that did not receive cells were used as negative controls and for determining the photography exposure settings.

For determining cell engraftment and migration, the number of DAPI/GFP-positive cells was determined along a distance of 1280 (640 μ m in each of the rostral and caudal directions from the transplantation site) at 4 hours and 10 days post-transplantation. Photographs were taken with a fluorescence Olympus IX70-S8F2 microscope with a fluorescent light source (excitation wavelength, 330–385 nm; barrier filter, 420 nm) and a U-MNU filter cube (Olympus).

Assessment of Neuromuscular Junction Innervations

Hind limb muscles were dissected and frozen in liquid nitrogen. Muscles were sectioned at 30 μ m using a cryostat and placed on glass slides for staining. Sections ($n = 10$ per animal) were fixed with 4% paraformaldehyde-PBS and labeled with α -bungarotoxin conjugated with fluorescence marker Alexa Fluor 594 (1:500; Invitrogen) and anti-synaptophysin (rabbit polyclonal, 1:500; Santa Cruz Biotechnology) antibodies overnight at 4°C. After washing with PBS, the sections were incubated with anti-rabbit Alexa Fluor 488-conjugated antibody (1:1,000; Invitrogen) for 1 hour at room temperature, followed by washes, and covered with cover glasses using aqueous mounting medium (Invitrogen). Cells incubated overnight with the blocking solution and then only with the secondary antibodies served as negative controls and for determining the photography exposure settings. We classified neuromuscular junctions (NMJs) into two groups based on the degree of innervation of postsynaptic receptor plaques by nerve terminals. Endplates were scored as innervated if there was an overlap

with the axon terminal, or denervated if the end plate was not associated with an axon.

Statistical Analysis

Results are expressed as mean \pm SEM. All analyses were performed using SPSS version 19 software (SPSS Software, IBM Corp., Armonk, NY, <http://www-01.ibm.com/software/analytics/spss/>). Differences between two groups were statistically analyzed by *t* test, whereas comparisons between three groups were analyzed by one-way analysis of variance (ANOVA). For the cell transplantation in vivo experiment, two-way ANOVA was performed. Tukey's multiple comparison post hoc test was used to evidence specific differences between groups.

RESULTS

Differentiated hOMSC Show an Astrocyte-Like Phenotype

Following the two-step differentiation protocol, the entire culture of differentiated hOMSC underwent substantial morphological changes to a neural-like morphology, resembling that of astrocytes (Fig. 1). The observed morphological changes included cell condensation from an initial fusiform morphology to the formation of multiple projections emerging from the cell body. These changes correlate with an increase in the expression of classical astrocyte markers GFAP, S100 β , and EAAT1 (GLAST) at the gene and protein levels, as evidenced by real-time PCR, immunofluorescence staining, and Western blots (Fig. 1). Moreover, differentiated hOMSC showed a significant reduction in the transcription levels of pluripotency markers OCT4 and NANOG ($p < .05$) and a moderate reduction in the neural crest marker p75^{NTR} and the neuronal markers β -III tubulin and NCAM1 ($p < .05$) as compared with undifferentiated hOMSC (Fig. 1E–1F). hOMSC differentiation into astrocyte-like cells resulted in enhanced expression of the neurotrophic factors BDNF, GDNF, IGF-1, and VEGF, as evidenced by immunofluorescence staining (Fig. 2). At mRNA level, VEGF and BDNF were also upregulated ($p < .05$) (Fig. 2Ba, 2Bb). VEGF and BDNF levels were substantially increased in the extracellular medium ($p < .05$), reaching concentrations of approximately 8 ng/ml per 10⁶ cells and 1 ng/ml per 10⁶ cells, respectively, as measured by ELISA (Fig. 2Bc, 2Bd).

Conditioned Medium of Differentiated hOMSC Protects Motor Neurons From Hypoxia and Oxidative Stress-Induced Cell Death In Vitro

To evaluate the potential of the differentiated cells to protect neuronal cultures from hypoxia and oxidative stress-induced cell death, the mouse motor neuron cell line NSC-34 [37] was used (Fig. 3). After 72 hours of hypoxia, cell viability in the untreated NSC-34 cultures and in NSC-34 treated with conditioned medium derived from naïve hOMSC decreased to 11.85% \pm 0.82% and 15.23% \pm 3.87% of the cell viability levels observed in NSC-34 cultures grown under normoxia ($p < .05$). In contrast, NSC-34 treated with conditioned medium from differentiated hOMSC cultures exhibited high survival rates (93.8% \pm 9%) comparable to those of NSC-34 cultures maintained under normoxia conditions ($p < .05$) (Fig. 3A). The survival rate of NSC-34 cultures exposed to oxidative stress (25 μ M H₂O₂) for 48 hours and treated with condition medium derived from differentiated hOMSC was similar to that of control cultures unexposed to oxidative

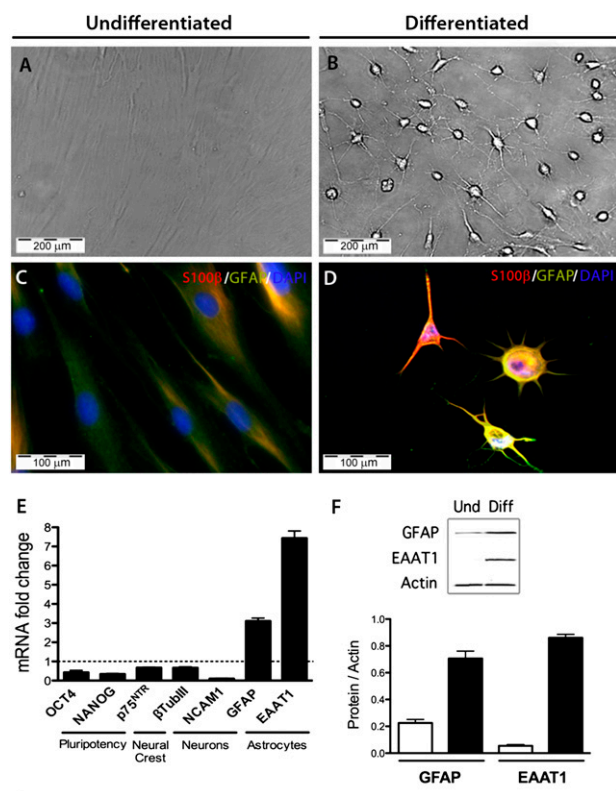


Figure 1. Differentiated human oral mucosa stem cells (hOMSC) exhibit an astrocyte-like phenotype. Bright field (A, B) and immunofluorescence microscopy (C, D) for S100 β (red) and GFAP (green) of undifferentiated and differentiated hOMSC (scale bars = 100 μ m). Decrease in the expression of pluripotency, neural crest, and neuronal markers and increase in the expression of the astrocytic markers GFAP and EAAT1 in differentiated hOMSC, as assessed by quantitative polymerase chain reaction (E). Confirmation of the increase observed in the astrocytic markers at the message level by quantitative Western blots (F). Abbreviations: DAPI, 4',6-diamidino-2-phenylindole; Diff, differentiated; EAAT1, excitatory amino acid transporter 1; GFAP, glial fibrillary acidic protein; NANOG, neural adhesion molecule; OCT4, octamer-binding transcription factor; Und, undifferentiated.

stress. The survival rate of cultures treated with conditioned medium from naïve hOMSC and that of untreated cultures was $83.47\% \pm 6.8\%$ and $65.88\% \pm 1.74\%$, respectively, of that of cultures unexposed to oxidative stress ($p < .05$) (Fig. 3B). Because of the neuroprotective capacity of the hOMSC-differentiated cells, they will be referred to in this work as hOMSC-derived neuron-supporting cells (hOMSC-NS).

hOMSC-NS Transplantation Increases Motor Performance After Sciatic Nerve Injury in Rats

The sciatic nerve injury model was used for testing the capacity of hOMSC-NS to support peripheral neural recovery (Fig. 4A). As demonstrated by the rotarod test, a significant improvement in the motor function was achieved in the animals of the hOMSC-NS-transplanted group during the first stages of recovery, compared with that of animals treated with naïve hOMSC or saline (Fig. 4C). This improvement was statistically significant ($p < .05$) between days 1 and 7 after cell transplantation. No differences in the improvement of motor function were observed between the saline-treated and the naïve hOMSC-treated groups ($p > .05$).

hOMSC-NS Engrafted and Maintained Their Phenotype In Vivo

To test the fate of the transplanted cells, the gastrocnemius muscle was examined by histochemistry and immunofluorescence staining. Prussian blue staining revealed the presence of the superparamagnetic iron oxide-positive cells in between and within the muscle bundles (data not shown). GFP⁺ naïve hOMSC and GFP⁺ hOMSC-NS were detected in the inoculated muscle 4 hours after transplantation and 10 days thereafter (Fig. 5). Quantitative analysis revealed that at 4 hours postinoculation most of the cells were localized in a perimeter of approximately 400 μ m. Serial section analysis revealed expansion of this territory by approximately 400 μ m in each of the rostral and caudal direction, pointing to a migratory process along the muscle fibers. Even though the amount of migration was similar for the two cell types, the naïve hOMSC migrated by 100 μ m more than the hOMSC-NS (Fig. 5H). The integrity of the human cells 10 days post-transplantation was confirmed by positive immunofluorescent staining of human nuclei with antibodies for the human nuclear antigen (HuNu) in the transplanted muscles. No signal was observed in the saline-injected muscles (Fig. 6D–6F). hOMSC-NS maintained their capacity to secrete NTF and their astrocyte-like phenotype in vivo, as evidenced by the expression of BDNF, VEGF, and GFAP, respectively (Fig. 6A–6F). Colocalization of GFAP and VEGF in the hOMSC-NS-transplanted muscles indicated that GFAP-positive cells are actively secreting VEGF 10 days following their transplantation in vivo. Furthermore, human nuclear antigen (HuNu) and BDNF were colocalized in hOMSC-NS-transplanted tissues, whereas such a finding was not observed in tissues transplanted with either naïve hOMSC or saline. A significant increase in BDNF signal in rats transplanted with hOMSC-NS as compared with rats transplanted with saline or naïve hOMSC was detected (Fig. 6D–6F). A low BDNF signal was also observed in sections of the control groups, probably because of endogenous BDNF synthesis by muscle progenitor cells [38, 39]. Notably, naïve hOMSC also expressed low levels of GFAP (Fig. 6B). Estimation of the GFAP-positive areas indicated that sections derived from hOMSC-NS-transplanted animals exhibited a 3.3- and 6-fold increase in relative fluorescence compared with sections obtained from naïve hOMSC and saline-treated animals, respectively ($p < .05$) (Fig. 6G). Similarly, the relative fluorescence of VEGF-positive areas in this section obtained from hOMSC-NS-treated animals was 13.8- and 16.6-fold higher than that observed in sections obtained from animals transplanted with naïve hOMSC or treated with saline, respectively ($p < .05$) (Fig. 6H). BDNF-positive areas exhibited a similar pattern, even though the differences in the relative fluorescence between the groups were smaller than those observed for GFAP and VEGF (Fig. 6I).

Transplanted hOMSC-NS Preserved Neuromuscular Junctions After Injury

Ten days after the sciatic nerve crush, NMJs were evaluated and counted within the gastrocnemius and tibialis muscles in the crushed area in animals of the three groups (Fig. 7). Colocalization of the presynaptic protein synaptophysin (SYP) (red) and of the postsynaptic acetylcholine receptor ligand, α -bungarotoxin (α -BTX) (green), pointed to preserved and innervated NMJ (yellow) (Fig. 7A–7I). Staining for either α -BTX or SYP alone was considered as a denervated NMJ. Evaluation of the NMJ was

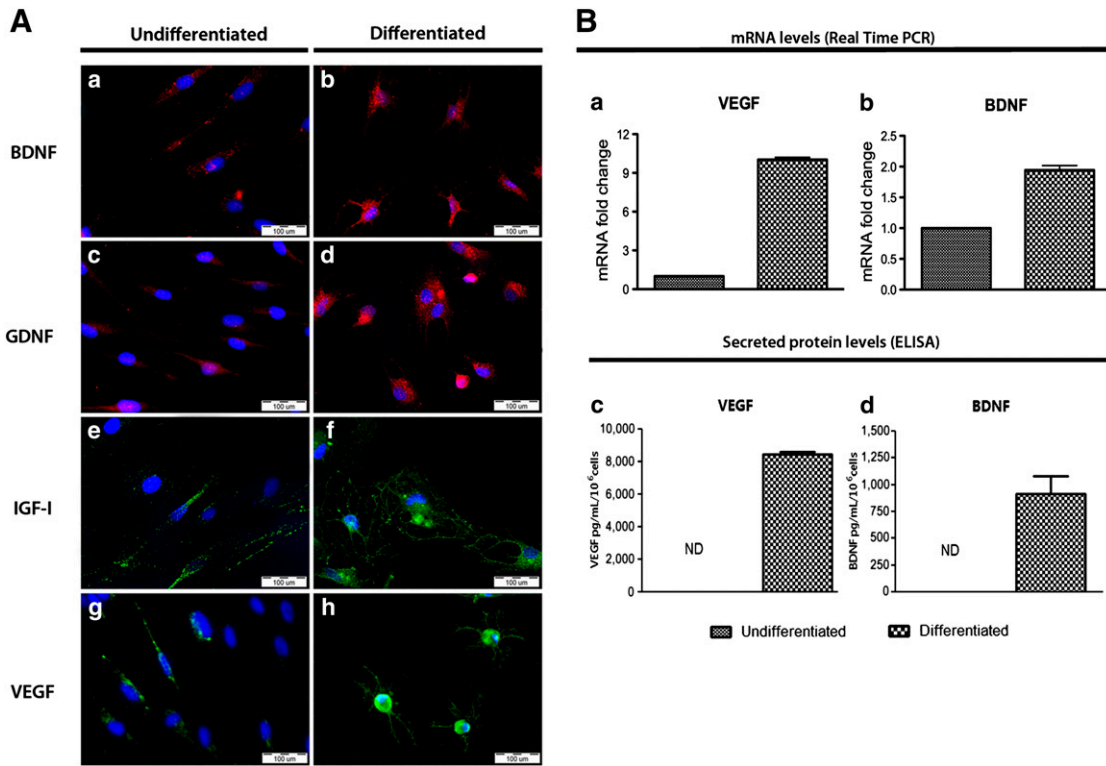


Figure 2. Differentiated human oral mucosa stem cells present enhanced neurotrophic factors (NTF) production and secretion. **(A):** Immunofluorescence of intracellular NTF before and after differentiation, BDNF, GDNF, IGF-1, and VEGF (**Aa–Ah**). Scale bars = 100 μ m. **(B):** VEGF and BDNF expression at the mRNA level (**Ba, Bb**) and secreted protein level (**Bc, Bd**) assessed by real-time PCR and enzyme-linked immunosorbent assay, respectively. Abbreviations: BDNF, brain-derived neurotrophic factor; GDNF, glial-derived neurotrophic factor; IGF-1, insulin-like growth factor 1; ND, not determined; PCR, polymerase chain reaction; VEGF, vascular endothelial growth factor.

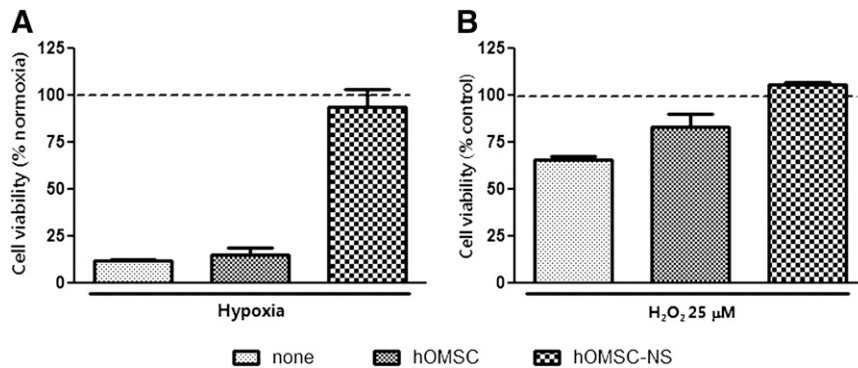


Figure 3. Differentiated hOMSC-conditioned medium protects motor neurons from hypoxia and oxidative stress. NSC34 cells incubated under hypoxic **(A)** or oxidative **(B)** conditions. Treatments include serum-free medium and conditioned medium from differentiated and undifferentiated hOMSC. Data are presented as percentage (mean \pm SEM) of cells without insult. Abbreviations: hOMSC, human oral mucosa stem cells; hOMSC-NS, human oral mucosa stem cells-neuronal support.

expressed as a percentage of preserved NMJ counts over total counted NMJ (α BTX⁺SYP⁺ + α BTX⁺ + SYP⁺). We found that in gastrocnemius and tibialis muscles transplanted with hOMSC-NS, 89.4% \pm 4.6% of the NMJs were innervated. In contrast, in muscles transplanted with hOMSC or saline only, 53.5% \pm 8.3% and 48.2% \pm 8% of the NMJs were innervated, respectively (Fig. 7J). Statistical analysis demonstrated significant difference between the hOMSC-NS-treated group and the other two groups, which did not differ from each other (ANOVA and Tukey’s post hoc analysis, $p < .05$).

DISCUSSION

Stem cell therapy is evolving as a promising strategy for the treatment of degenerative and traumatic disorders of the central and peripheral nervous systems. To establish reproducible therapeutic protocols, similar to those accepted in drug therapy, therapeutic stem cell populations with a well-characterized phenotype must be developed and used. Allogeneic embryonic and fetal well-characterized stem cell lines are currently being tested in preclinical [40] and clinical settings [41, 42]. However,

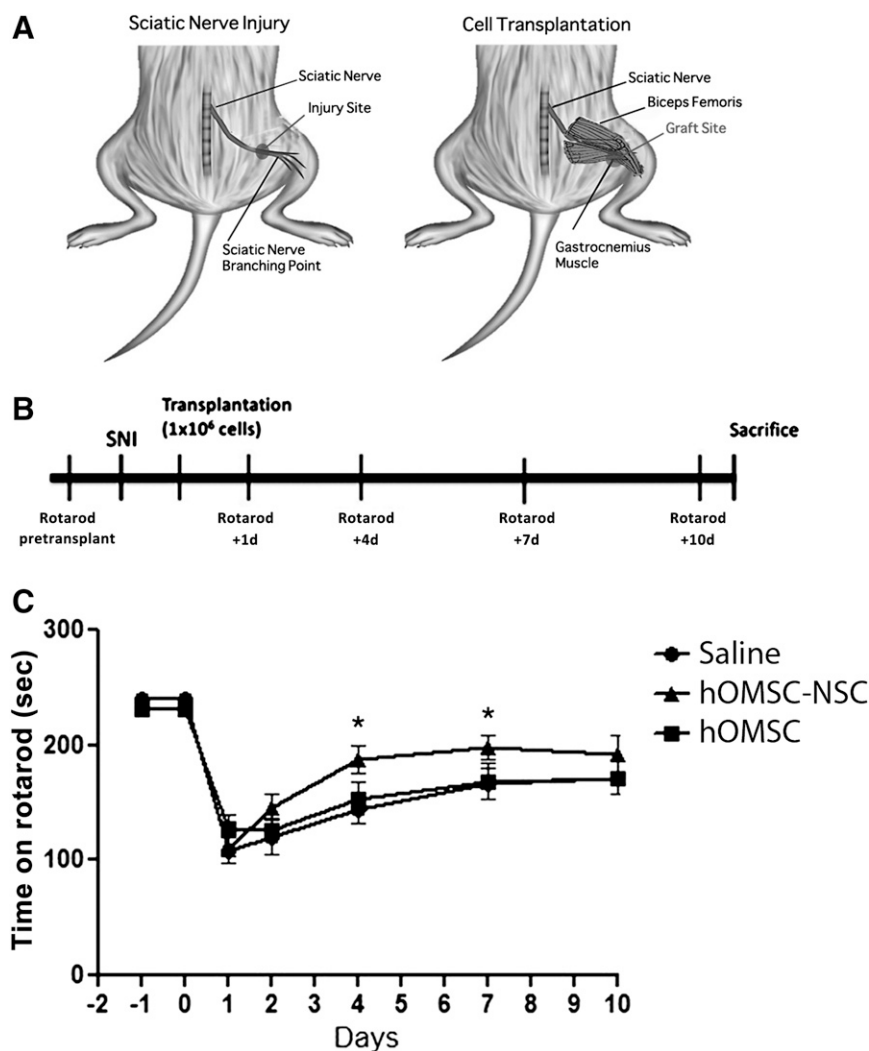


Figure 4. Transplanted human oral mucosa stem cells-neuronal support (hOMSC-NS) improve motor behavior of sciatic nerve-injured rats. **(A):** Diagram of sciatic nerve injury and cell transplantation performed in rats. **(B):** Diagram of the protocol used for cell transplantation and evaluation time points. **(C):** Motor analysis of transplanted rats with hOMSC-NS, hOMSC, and saline ($n = 8$ per group). Motor function was assessed by rotarod and is presented as time spent on the rod (seconds). Data are presented as mean \pm SEM, analysis of variance repeated measures ($p = .0261$). Abbreviations: hOMSC, human oral mucosa stem cells; hOMSC, human oral mucosa-derived neuronal supporting cells; SNI, sciatic nerve injury.

immunologic, ethical, and safety issues still hamper their routine utilization. Autologous adult stem cells, derived from bone marrow [30, 43–45] or other sources [12, 46–48], have recently been coaxed by exposure to soluble factors or genetic manipulations to produce and secrete specific trophic factors with biologic activities. These cells have also been shown to ameliorate functional symptoms in animal models of trauma and neurodegenerative diseases [18, 28, 47–50]. However, the donor heterogeneity and aging may affect the outcome of the differentiation protocols and consequently the therapeutic efficacy of these stem cell populations [51–53]. In this respect, we have recently reported that hOMSC are a unique population of multipotent stem cells with a primitive NC-like phenotype [32]. hOMSC are localized within a specific niche in the NC-derived lamina propria of the adult and elderly oral mucosa. Moreover, hOMSC express low interdonor heterogeneity, and their growth, clonogenicity, and differentiation potentials are negligibly affected by aging [32].

The NC gives rise to a wide range of cell types, including neurons and glia of the PNS, melanocytes, craniofacial bones and cartilage, fibroblasts, smooth muscle cells, and endocrine cells [34]. Migrating NC cells are a heterogeneous collection of progenitors, including multipotent stem cells, cells with limited developmental potential, and fate-restricted precursors [34]. The influence of environmental signals is therefore crucial to ensure that postmigratory NC-derived cells express a defined phenotype corresponding to their position in the body. It was shown that the plasticity displayed by NC-derived cells is also retained postnatally by some differentiated cells. The idea of reprogramming NC phenotypes is supported by in vitro culture experiments that illustrate the ability of epidermal pigment cells and peripheral nerve Schwann cells, two differentiated NC-derived cells, isolated from quail embryos, to undergo reciprocal transdifferentiation [34, 35, 54].

Considering that the NC in development gives rise to neuronal supporting cells such as satellite glial cells of the ganglia or the

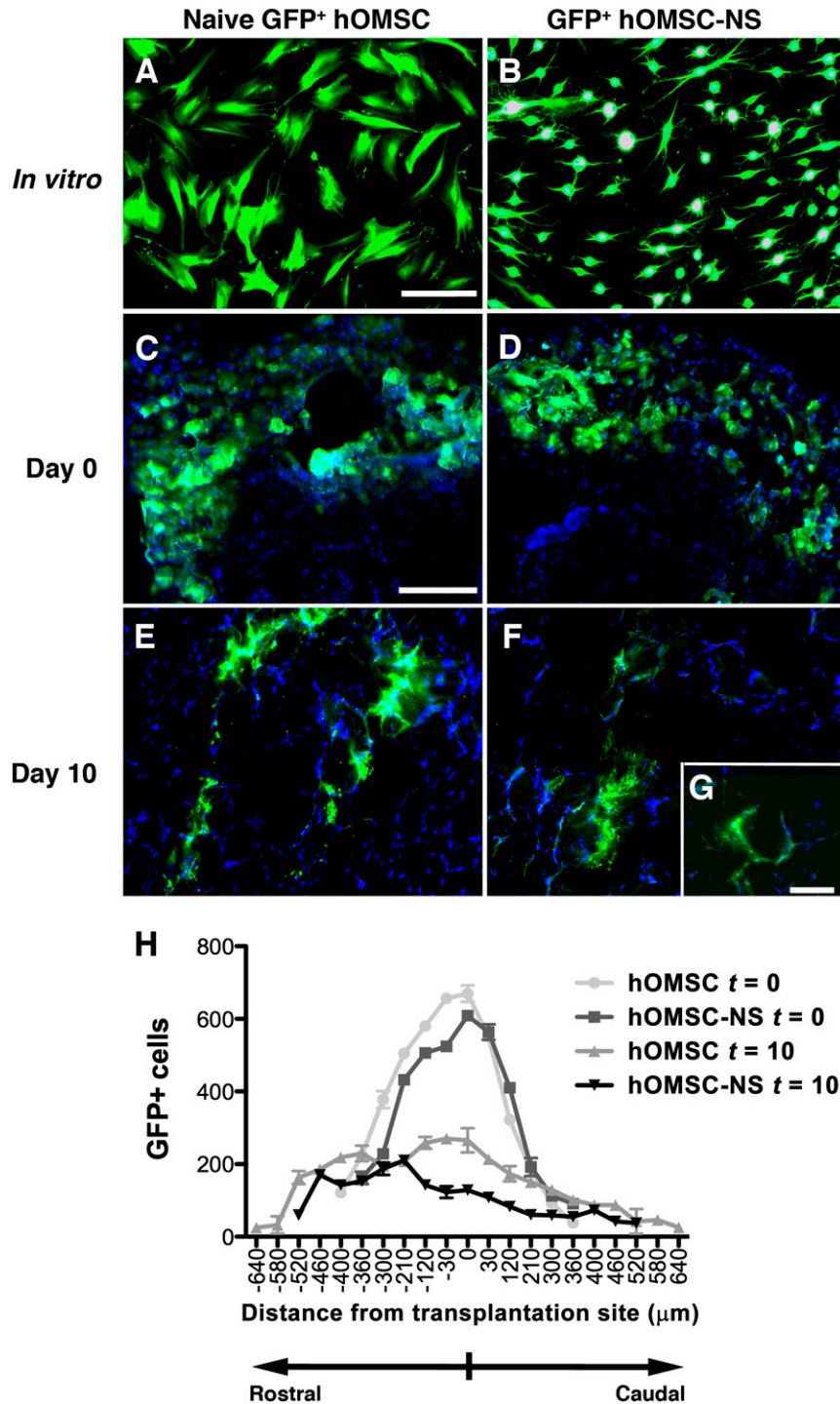


Figure 5. Transplanted cells survived 10 days after transplantation. GFP-labeled naïve or differentiated hOMSC (**A, B**) (scale bar = 100 μm) were transplanted into rats with sciatic nerve injury (*n* = 6). Cell survival was evaluated 4 hours (*t* = 0) and 10 days (*t* = 10) after transplantation (**C–F**). Scale bars = 200 μm (**C–F**) and 50 μm (**G**). GFP⁺ cells were counted and graphed as number of cells per section (30 μm) along 1280 μm rostro-caudal consecutive sections (0 μm refers to the inoculation site) (**H**). Abbreviations: GFP, green fluorescent protein; hOMSC, human oral mucosa stem cells; hOMSC-NS, human oral mucosa stem cells-neuronal support.

enteric glia [33], and given the remarkable plasticity of NC-derived cells, we set out to test the propensity of this cell population to differentiate into glial cells with in vitro and in vivo neuroprotective capacity, mimicking astrocytes' trophic and protective functions. It was demonstrated that neuregulin, or so-called

heregulin, is involved in determination, proliferation, differentiation, and migration of glial cells in the developing brain, and also in promoting selective maturation and cell viability of astrocytes [55, 56]. PDGF also regulates astrocyte specification by the leukemia inhibitory factor and bone morphogenetic protein 2 pathways

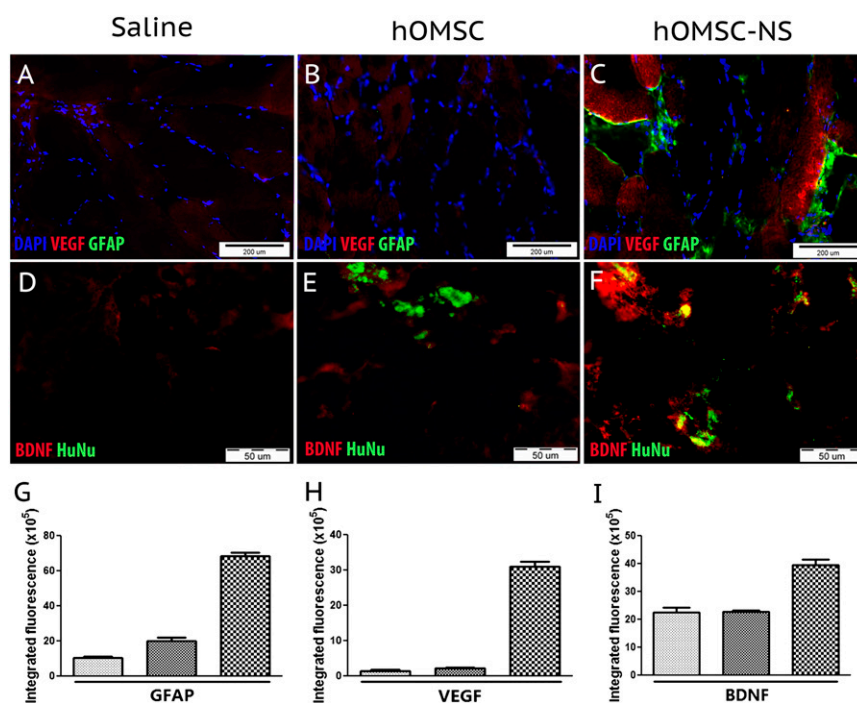


Figure 6. hOMSC-NS maintain phenotype and neurotrophic factor secretion in vivo. Immunofluorescence sections of the gastrocnemius muscle obtained 10 days post-transplantation. Columns represent different transplanted groups (saline, naive, and differentiated hOMSC). First row illustrated staining for GFAP/VEGF/DAPI (A–C) and second row for HuNu/BDNF (D–F). Scale bars = 200 μ m. Fluorescence emission analysis of GFAP, VEGF, and BDNF intensity (G–I). Abbreviations: BDNF, brain-derived neurotrophic factor; DAPI, 4',6-diamidino-2-phenylindole; GFAP, glial fibrillary acidic protein; hOMSC, human oral mucosa stem cells; hOMSC-NS, human oral mucosa stem cells-neuronal support; HuNu, human nuclei; VEGF, vascular endothelial growth factor.

[57]. Addition of fibroblast growth factor-2 (FGF-2) in vitro provides a permissive environment for the production of astrocytes from cortical progenitors via multiple mechanisms, including the ciliary neurotrophic factor signaling, which is a major astroglial pathway [58–61]. Injection of FGF-2 into the cerebral ventricles of embryos and genetic manipulation to eliminate FGF-2 resulted in increased and decreased glial populations, demonstrating that FGF-2 signaling pathways induce and regulate astrocyte specification [58, 62, 63]. cAMP enhance FGF-2 and EGF expression but also induce the expression of the glutamate transporter EAAT1 (Glast) [64, 65]. Moreover, cAMP and IBMX were shown to induce the expression of NTF in primary astrocyte cultures [66].

In this study, we demonstrate that soluble factors, related to astrocyte differentiation, maturation, and increased NTF production, induced hOMSC homogenous differentiation into cells with induced upregulation of astrocyte markers, enhanced NTF secretion, and acquired neuroprotective capabilities.

The level of NTF secretion achieved after differentiation was comparable with those we published for myogenic cells transduced with viral vectors that effectively protected the sciatic nerve after injury [47]. Moreover, VEGF secretion by hOMSC-NS was even higher than myogenic progenitors transduced to express this cytokine [47].

A major concern in cell therapy is the capacity of the differentiated cells in vitro to survive and maintain their phenotype following their transplantation in vivo. In the present work, we demonstrated that a considerable number of both cell types survived for at least 10 days, the critical period for neural regeneration in this model. Moreover, we could detect higher amounts of GFAP, VEGF, and BDNF in the muscle transplanted with hOMSC-

NS compared with the other two groups. This observation correlated positively with motor and NMJ preservation. The findings that a higher expression of NTF was observed in hOMSC-NS-treated rats and that this secretion was colocalized with the astrocyte marker GFAP and also with cells of human origin point to the capacity of hOMSC-NS to maintain their astrocyte-like phenotype in vivo within the limit of the experimental period. We could not detect colocalization staining for GFAP and HuNu because of technical limitations.

The astrocyte-like phenotype of hOMSC-NS proved to have functional activity both in vitro and in vivo, as evidenced by their ability to rescue motor neurons subjected to chemical and respiratory stress, and by the ability to preserve NMJ innervation and enhance functional recovery of sciatic nerve-injured rats. The fact that this functional activity correlates with increased secretion of NTF by hOMSC strengthens previous observations that glial-like cells derived from extraneural adult tissues protect and support neuronal function via the continuous secretion of soluble NTF [15, 19, 30].

Oral mucosa is a readily accessible cell source. Biopsies as small as $4\text{--}3 \times 3 \times 1$ mm generate under regular culture conditions trillions of hOMSC with a substantial propensity to differentiate into homogenous cultures of astrocyte-like cells. Preliminary results (data not shown) suggest that this propensity is negligibly affected by the age of the donor. Taken together, the data of the present and previous studies, showing that hOMSC are capable of developing into Schwann-like cells 2 months following their transplantation into severe combined immunodeficient mice [32], indicate that the oral mucosa might serve as an advantageous cell source for isolating therapeutic quantities of stem cells with

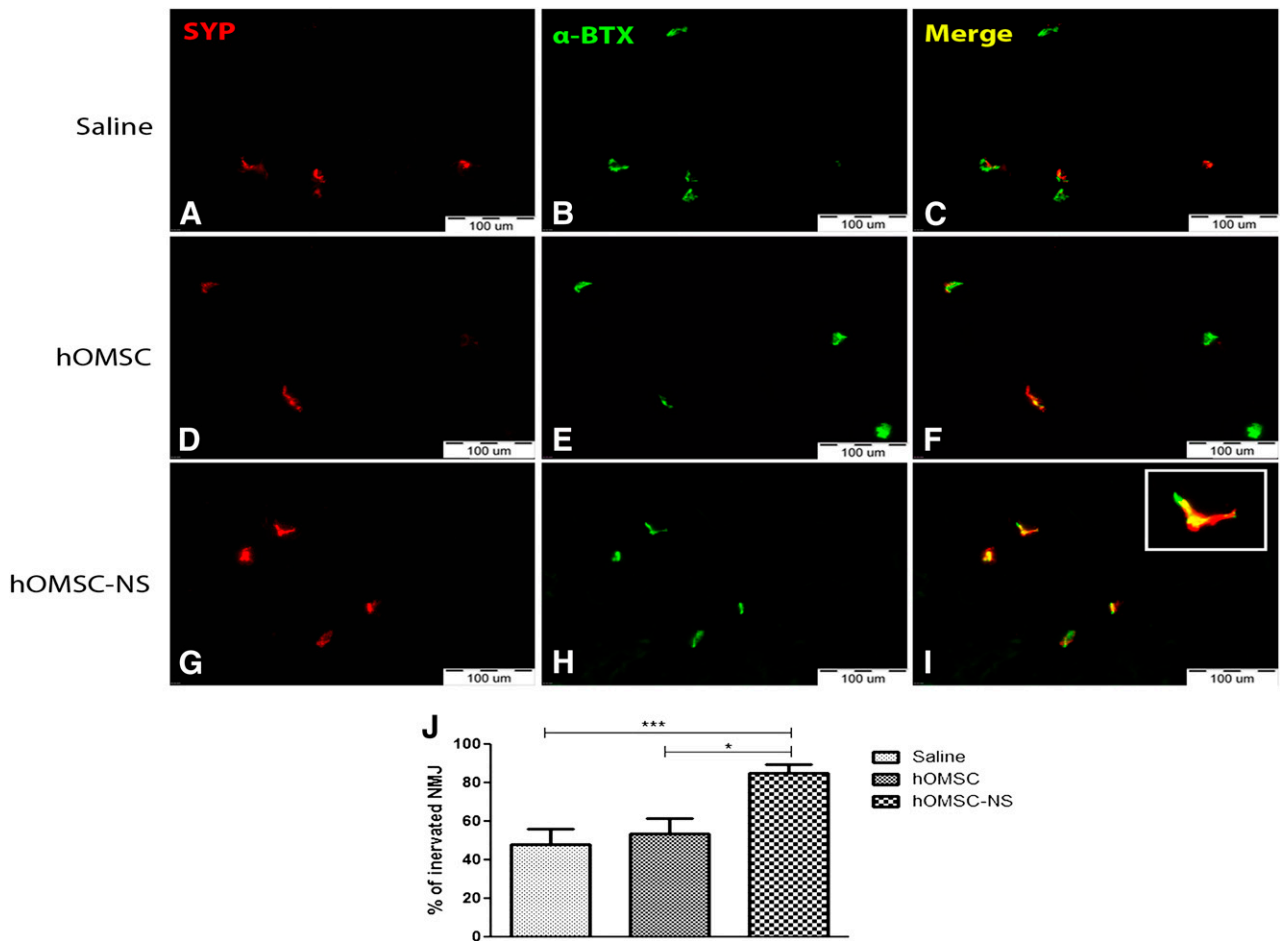


Figure 7. Transplanted hOMSC-NS preserved functional NMJs. Hind limb muscle sections of the three experimental groups (A–I) obtained 10 days post-transplantation. Colocalization of α -bungarotoxin (green) and synaptophysin (red) detects functional NMJ (yellow). Scale bars = 100 μ m. Quantification of NMJs (J) is expressed as percentage of preserved NMJ (α -BTX⁺SYP⁺) over total (α -BTX⁺SYP⁺ + α -BTX⁺ + SYP⁺). Data presented as mean \pm SEM. Abbreviations: α -BTX, α -bungarotoxin; hOMSC, human oral mucosa stem cells; hOMSC-NS, human oral mucosa stem cells-neuronal support; NMJ, neuromuscular junctions; SYP, synaptophysin.

a high propensity to differentiate along glial lineages and providing a neuronal support function similar to glial cells of the nervous system.

To conceive hOMSC-NS as a general neuroprotective strategy, a number of issues remain to be elucidated in further studies. (a) Cell survival at the graft site remains to be elucidated. (b) The behavior and fate of the transplanted cells for longer time periods remain to be addressed. (c) The mechanisms involved in the observed motor recovery and in the neuromuscular synaptic preservation remain to be elucidated. (d) hOMSC used in the present study were obtained from relatively young and healthy donors. Our preliminary results (data not shown) indicate that donor aging does not affect the basic properties of hOMSC such as proliferation and their capacity to differentiate in vitro. However, it is unknown whether aging or other inherited or acquired diseases of the donor affect their functionality in vivo. It also remains to be established whether hOMSC can be used for allogeneic transplantation. (e) In the present study, hOMSC were tested in a model of injured but young animals. It remains to be established how the age of the host affects the function of hOMSC-NS in vivo.

CONCLUSION

Our findings show for the first time that astrocyte-like cells with enhanced neurotrophic factor secretion and neuroprotective abilities can be successfully obtained through hOMSC differentiation. Considering the many advantages of using oral mucosa stem cells and the results shown in this work, hOMSC emerge as a novel stem cell population for autologous cell therapy of peripheral nerve injuries and possibly other neuropathies.

ACKNOWLEDGMENTS

We thank Dr. Igor Tarasenko for assistance with the animal model and Veronica Silva for editorial assistance. This work was performed in partial fulfillment of the requirements for a degree of Javier Ganz, Sackler Faculty of Medicine, Tel Aviv University. This work was supported, in part, by Binational United States–Israel Science Foundation (Grant 2007049 to S. Pitaru.), Israel Science Foundation of the Israeli Academy of Science (Grant 646/09 to S. Pitaru), and Ministry of Immigrant Absorption and SAIA Doctoral Prize and Scholarship Fund for Research fellowship (to J.G.).

AUTHOR CONTRIBUTIONS

J.G.: conception and design, collection and/or assembly of data, data analysis and interpretation, manuscript writing, final approval of manuscript; I.A.: collection and/or assembly of data; T.B.-Z.: collection and/or assembly of data, data analysis and interpretation; M.D.-N.: data analysis and interpretation; S. Pour and S.A.: provision of study material or patients; S. Pitaru: conception and design, data analysis and interpretation, manuscript writing, financial support, final approval of manuscript; D.O.:

conception and design, financial support, data analysis and interpretation, final approval of manuscript.

DISCLOSURE OF POTENTIAL CONFLICTS OF INTEREST

J.G. is an uncompensated patent holder. S. Pitaru is an uncompensated patent holder. D.O. is an uncompensated patent holder and compensated consultant with brainstorm cell therapeutics.

REFERENCES

- Ganz J, Lev N, Melamed E et al. Cell replacement therapy for Parkinson's disease: How close are we to the clinic? *Expert Rev Neurother* 2011;11:1325–1339.
- Kimelberg HK, Nedergaard M. Functions of astrocytes and their potential as therapeutic targets. *Neurotherapeutics* 2010;7:338–353.
- Yamanaka K, Boillee S, Roberts EA et al. Mutant SOD1 in cell types other than motor neurons and oligodendrocytes accelerates onset of disease in ALS mice. *Proc Natl Acad Sci USA* 2008;105:7594–7599.
- Barbeito LH, Pehar M, Cassina P et al. A role for astrocytes in motor neuron loss in amyotrophic lateral sclerosis. *Brain Res Brain Res Rev* 2004;47:263–274.
- Miquel E, Cassina A, Martínez-Palma L et al. Modulation of astrocytic mitochondrial function by dichloroacetate improves survival and motor performance in inherited amyotrophic lateral sclerosis. *PLoS One* 2012;7:e34776.
- Díaz-Amarilla P, Olivera-Bravo S, Trias E et al. Phenotypically aberrant astrocytes that promote motoneuron damage in a model of inherited amyotrophic lateral sclerosis. *Proc Natl Acad Sci USA* 2011;108:18126–18131.
- Nakajima K, Hida H, Shimano Y et al. GDNF is a major component of trophic activity in DA-depleted striatum for survival and neurite extension of DAergic neurons. *Brain Res* 2001;916:76–84.
- Berglöv E, Af Bjerkén S, Strömberg I. Glial influence on nerve fiber formation from rat ventral mesencephalic organotypic tissue cultures. *J Comp Neurol* 2007;501:431–442.
- L'Episcopo F, Tirolo C, Testa N et al. Glia as a turning point in the therapeutic strategy of Parkinson's disease. *CNS Neurol Disord Drug Targets* 2010;9:349–372.
- Faulkner JR, Herrmann JE, Woo MJ et al. Reactive astrocytes protect tissue and preserve function after spinal cord injury. *J Neurosci* 2004;24:2143–2155.
- Franklin RJ, Blakemore WF. Glial-cell transplantation and plasticity in the O-2A lineage—implications for CNS repair. *Trends Neurosci* 1995;18:151–156.
- Lepore AC, Rauck B, Dejea C et al. Focal transplantation-based astrocyte replacement is neuroprotective in a model of motor neuron disease. *Nat Neurosci* 2008;11:1294–1301.
- Sofroniew MV, Vinters HV. Astrocytes: Biology and pathology. *Acta Neuropathol* 2010;119:7–35.
- Gritti A, Bonfanti L. Neuronal-glial interactions in central nervous system neurogenesis: The neural stem cell perspective. *Neuron Glia Biol* 2007;3:309–323.
- Sadan O, Bahat-Stromza M, Barhum Y et al. Protective effects of neurotrophic factor-secreting cells in a 6-OHDA rat model of Parkinson disease. *Stem Cells Dev* 2009;18:1179–1190.
- Sadan O, Melamed E, Offen D. Bone-marrow-derived mesenchymal stem cell therapy for neurodegenerative diseases. *Expert Opin Biol Ther* 2009;9:1487–1497.
- Sadan O, Shemesh N, Cohen Y et al. Adult neurotrophic factor-secreting stem cells: A potential novel therapy for neurodegenerative diseases. *Isr Med Assoc J* 2009;11:201–204.
- Bahat-Stroomza M, Barhum Y, Levy YS et al. Induction of adult human bone marrow mesenchymal stromal cells into functional astrocyte-like cells: Potential for restorative treatment in Parkinson's disease. *J Mol Neurosci* 2009;39:199–210.
- Dadon-Nachum M, Sadan O, Srugo I et al. Differentiated mesenchymal stem cells for sciatic nerve injury. *Stem Cell Rev* 2011;7:664–671.
- Xiong N, Zhang Z, Huang J et al. VEGF-expressing human umbilical cord mesenchymal stem cells, an improved therapy strategy for Parkinson's disease. *Gene Ther* 2011;18:394–402.
- Kitiyanant N, Kitiyanant Y, Svendsen CN et al. BDNF, IGF-1- and GDNF-secreting human neural progenitor cells rescue amyloid β -induced toxicity in cultured rat septal neurons. *Neurochem Res* 2012;37:143–152.
- Ozdinler PH, Macklis JD. IGF-I specifically enhances axon outgrowth of corticospinal motor neurons. *Nat Neurosci* 2006;9:1371–1381.
- Dobrowolny G, Giacinti C, Pelosi L et al. Muscle expression of a local Igf-1 isoform protects motor neurons in an ALS mouse model. *J Cell Biol* 2005;168:193–199.
- Azzouz M, Ralph GS, Storkebaum E et al. VEGF delivery with retrogradely transported lentivector prolongs survival in a mouse ALS model. *Nature* 2004;429:413–417.
- Zheng C, Sköld MK, Li J et al. VEGF reduces astrogliosis and preserves neuromuscular junctions in ALS transgenic mice. *Biochem Biophys Res Commun* 2007;363:989–993.
- Acsadi G, Anguelov RA, Yang H et al. Increased survival and function of SOD1 mice after glial cell-derived neurotrophic factor gene therapy. *Hum Gene Ther* 2002;13:1047–1059.
- Mohajeri MH, Figlewicz DA, Bohn MC. Intramuscular grafts of myoblasts genetically modified to secrete glial cell line-derived neurotrophic factor prevent motoneuron loss and disease progression in a mouse model of familial amyotrophic lateral sclerosis. *Hum Gene Ther* 1999;10:1853–1866.
- Barhum Y, Gai-Castro S, Bahat-Stromza M et al. Intracerebroventricular transplantation of human mesenchymal stem cells induced to secrete neurotrophic factors attenuates clinical symptoms in a mouse model of multiple sclerosis. *J Mol Neurosci* 2010;41:129–137.
- Fisher-Shoval Y, Barhum Y, Sadan O et al. Transplantation of placenta-derived mesenchymal stem cells in the EAE mouse model of MS. *J Mol Neurosci* 2012;48:176–184.
- Sadan O, Shemesh N, Barzilay R et al. Mesenchymal stem cells induced to secrete neurotrophic factors attenuate quinolinic acid toxicity: A potential therapy for Huntington's disease. *Exp Neurol* 2012;234:417–427.
- Levkovitch-Verbin H, Sadan O, Vander S et al. Intravitreal injections of neurotrophic factors secreting mesenchymal stem cells are neuroprotective in rat eyes following optic nerve transection. *Invest Ophthalmol Vis Sci* 2010;51:6394–6400.
- Marynka-Kalmani K, Treves S, Yafee M et al. The lamina propria of adult human oral mucosa harbors a novel stem cell population. *STEM CELLS* 2010;28:984–995.
- Le Douarin N, Dulac C, Dupin E et al. Glial cell lineages in the neural crest. *Glia* 1991;4:175–184.
- Le Douarin NM, Creuzet S, Couly G et al. Neural crest cell plasticity and its limits. *Development* 2004;131:4637–4650.
- Dupin E, Real C, Glavieux-Pardanaud C et al. Reversal of developmental restrictions in neural crest lineages: Transition from Schwann cells to glial-melanocytic precursors in vitro. *Proc Natl Acad Sci USA* 2003;100:5229–5233.
- Davies LC, Locke M, Webb RD et al. A multipotent neural crest-derived progenitor cell population is resident within the oral mucosa lamina propria. *Stem Cells Dev* 2010;19:819–830.
- Durham HD, Dahrouge S, Cashman NR. Evaluation of the spinal cord neuron X neuroblastoma hybrid cell line NSC-34 as a model for neurotoxicity testing. *Neurotoxicology* 1993;14:387–395.
- Mousavi K, Jasmin BJ. BDNF is expressed in skeletal muscle satellite cells and inhibits myogenic differentiation. *J Neurosci* 2006;26:5739–5749.
- Clow C, Jasmin BJ. Brain-derived neurotrophic factor regulates satellite cell differentiation and skeletal muscle regeneration. *Mol Biol Cell* 2010;21:2182–2190.
- Lu B, Malcuit C, Wang S et al. Long-term safety and function of RPE from human embryonic stem cells in preclinical models of macular degeneration. *STEM CELLS* 2009;27:2126–2135.

- 41 Schwartz SD, Hubschman JP, Heilwell G et al. Embryonic stem cell trials for macular degeneration: A preliminary report. *Lancet* 2012; 379:713–720.
- 42 Pitaru S, Savion N, Hekmati H et al. Molecular and cellular interactions of a cementum attachment protein with periodontal cells and cementum matrix components. *J Periodontol Res* 1993;28:560–562.
- 43 Suzuki M, McHugh J, Tork C et al. Direct muscle delivery of GDNF with human mesenchymal stem cells improves motor neuron survival and function in a rat model of familial ALS. *Mol Ther* 2008;16:2002–2010.
- 44 Dezawa M. Systematic neuronal and muscle induction systems in bone marrow stromal cells: The potential for tissue reconstruction in neurodegenerative and muscle degenerative diseases. *Med Mol Morphol* 2008;41:14–19.
- 45 Shimizu S, Kitada M, Ishikawa H et al. Peripheral nerve regeneration by the in vitro differentiated-human bone marrow stromal cells with Schwann cell property. *Biochem Biophys Res Commun* 2007;359:915–920.
- 46 Mohajeri M, Farazmand A, Mohyeddin Bonab M et al. FOXP3 gene expression in multiple sclerosis patients pre- and post mesenchymal stem cell therapy. *Iran J Allergy Asthma Immunol* 2011;10:155–161.
- 47 Dadon-Nachum MB-ZT, Srugo I, Shamir H M, Melamed E, Yaffe D, Offen D. Therapeutic effect of myogenic cells modified to express neurotrophic factors in a rat model of sciatic nerve injury. *Journal of Stem Cells and Regenerative Medicine* 2012;8:22–26.
- 48 Jin Y, Neuhuber B, Singh A et al. Transplantation of human glial restricted progenitors and derived astrocytes into a contusion model of spinal cord injury. *J Neurotrauma* 2011;28: 579–594.
- 49 Lepore AC, O'Donnell J, Kim AS et al. Human glial-restricted progenitor transplantation into cervical spinal cord of the SOD1 mouse model of ALS. *PLoS One* 2011;6:e25968.
- 50 Dadon-Nachum M, Melamed E, Offen D. Stem cells treatment for sciatic nerve injury. *Expert Opin Biol Ther* 2011;11:1591–1597.
- 51 Stenderup K, Justesen J, Clausen C et al. Aging is associated with decreased maximal life span and accelerated senescence of bone marrow stromal cells. *Bone* 2003;33:919–926.
- 52 Zhou S, Greenberger JS, Epperly MW et al. Age-related intrinsic changes in human bone-marrow-derived mesenchymal stem cells and their differentiation to osteoblasts. *Aging Cell* 2008;7:335–343.
- 53 Stolzing A, Jones E, McGonagle D et al. Age-related changes in human bone marrow-derived mesenchymal stem cells: Consequences for cell therapies. *Mech Ageing Dev* 2008; 129:163–173.
- 54 Dupin E, Glavieux C, Vaigot P et al. Endothelin 3 induces the reversion of melanocytes to glia through a neural crest-derived glial-melanocytic progenitor. *Proc Natl Acad Sci USA* 2000;97:7882–7887.
- 55 Pinkas-Kramarski R, Eilam R, Spiegler O et al. Brain neurons and glial cells express Neu differentiation factor/heredulin: A survival factor for astrocytes. *Proc Natl Acad Sci USA* 1994; 91:9387–9391.
- 56 Kerber G, Streif R, Schwaiger FW et al. Neuregulin-1 isoforms are differentially expressed in the intact and regenerating adult rat nervous system. *J Mol Neurosci* 2003;21:149–165.
- 57 Adachi T, Takanaga H, Kunimoto M et al. Influence of LIF and BMP-2 on differentiation and development of glial cells in primary cultures of embryonic rat cerebral hemisphere. *J Neurosci Res* 2005;79:608–615.
- 58 Kang K, Song MR. Diverse FGF receptor signaling controls astrocyte specification and proliferation. *Biochem Biophys Res Commun* 2010;395:324–329.
- 59 Qian X, Davis AA, Goderie SK et al. FGF2 concentration regulates the generation of neurons and glia from multipotent cortical stem cells. *Neuron* 1997;18:81–93.
- 60 Song MR, Ghosh A. FGF2-induced chromatin remodeling regulates CNTF-mediated gene expression and astrocyte differentiation. *Nat Neurosci* 2004;7:229–235.
- 61 Ravin R, Hoepfner DJ, Munno DM et al. Potency and fate specification in CNS stem cell populations in vitro. *Cell Stem Cell* 2008;3: 670–680.
- 62 Raballo R, Rhee J, Lyn-Cook R et al. Basic fibroblast growth factor (Fgf2) is necessary for cell proliferation and neurogenesis in the developing cerebral cortex. *J Neurosci* 2000;20: 5012–5023.
- 63 Vaccarino FM, Schwartz ML, Raballo R et al. Changes in cerebral cortex size are governed by fibroblast growth factor during embryogenesis. *Nat Neurosci* 1999;2:848.
- 64 Stanimirovic DB, Ball R, Small DL et al. Developmental regulation of glutamate transporters and glutamine synthetase activity in astrocyte cultures differentiated in vitro. *Int J Dev Neurosci* 1999;17:173–184.
- 65 Bayatti N, Engele J. Cyclic AMP differentially regulates the expression of fibroblast growth factor and epidermal growth factor receptors in cultured cortical astroglia. *Neuroscience* 2002;114:81–89.
- 66 Condorelli DF, Dell'Albani P, Mudò G et al. Expression of neurotrophins and their receptors in primary astroglial cultures: Induction by cyclic AMP-elevating agents. *J Neurochem* 1994;63:509–516.

This article, along with others on similar topics, appears in the following collection(s):

Neural/Progenitor Stem Cells

<http://stemcellstm.alphamedpress.org/cgi/collection/neural-progenitor-stem-cells> **Tissue Engineering and Regenerative Medicine**

<http://stemcellstm.alphamedpress.org/cgi/collection/tissue-engineering-and-regenerative-medicine>

**Astrocyte-Like Cells Derived From Human Oral Mucosa Stem Cells Provide
Neuroprotection In Vitro and In Vivo**
Javier Ganz, Ina Arie, Tali Ben-Zur, Michal Dadon-Nachum, Sammy Pour, Shareef
Araidy, Sandu Pitaru and Daniel Offen

Stem Cells Trans Med 2014, 3:375-386.
doi: 10.5966/sctm.2013-0074 originally published online January 29, 2014

The online version of this article, along with updated information and services, is
located on the World Wide Web at:
<http://stemcellstm.alphamedpress.org/content/3/3/375>